frontiers | Frontiers in Chemistry

TYPE Review
PUBLISHED 26 September 2022
DOI 10.3389/fchem.2022.1023003

OPEN ACCESS

EDITED BY
Hongda Li,
Guangxi University of Science and Technology, China

REVIEWED BY
Xintong Liu,
Beijing Technology and Business University, China
Zhanglei Ning,
Sichuan Normal University, China

*CORRESPONDENCE
Shaonan Gu,
sngu@qlu.edu.cn
Guowei Zhou,
gwzhou@qlu.edu.cn

SPECIALTY SECTION
This article was submitted to Electrochemistry, a section of the journal Frontiers in Chemistry

RECEIVED 19 August 2022
ACCEPTED 31 August 2022
PUBLISHED 26 September 2022

CITATION
Guo M, Gu S, Xu S, Lu J, Wang Y and Zhou G (2022), Design, synthesis and application of two-dimensional metal tellurides as high-performance electrode materials.
Front. Chem. 10:1023003.
doi: 10.3389/fchem.2022.1023003

Design, synthesis and application of two-dimensional metal tellurides as high-performance electrode materials

Meng Guo, Shaonan Gu*, Shuzheng Xu, Jiani Lu, Yinan Wang and Guowei Zhou*

Key Laboratory of Fine Chemicals in Universities of Shandong, Jinan Engineering Laboratory for Multi-scale Functional Materials, School of Chemistry and Chemical Engineering, Qilu University of Technology (Shandong Academy of Sciences), Jinan, China

Multifunctional electrode materials with inherent conductivity have attracted extensive attention in recent years. Two-dimensional (2D) metal telluride nanomaterials are more promising owing to their strong metallic properties and unique physical/chemical merits. In this review, recent advancements in the preparation of 2D metal tellurides and their application in electrode materials are presented. First, the most available preparation methods, such as hydro/solvent thermal, chemical vapor deposition, and electrodeposition, are summarized. Then, the unique performance of metal telluride electrodes in capacitors, anode materials of Li/Na ion batteries, electrocatalysis, and lithium-sulfur batteries are discussed. Finally, significant challenges and opportunities in the preparation and application of 2D metal tellurides are proposed.

KEYWORDS

2D metal tellurides, synthesis, electrocatalysis, batteries, electrodes

1 Introduction

Increasing concerns about scarce resources and global climate issues have promoted the pursuit of clean and renewable energy for all humanity (Goodenough, 2014; Zeng et al., 2019). Many initiatives have attempted to power industrial civilization with renewable energy while ensuring the economic viability of related technologies, such as supercapacitors (SCs), alkali-ion batteries, lithium-sulfur (Li-S) batteries, etc., (Jaiswal, 2017; Zhang and Guo, 2020; Elmorshedy et al., 2021). Since then, electrode materials have emerged as a popular research topic in recent years. Many studies have attempted to improve the electrochemical characteristics of electrode materials by changing their composition, nano/microstructures, electronic properties, and so on (Zhang et al., 2019a; Zheng et al., 2021). However, as electrodes, one of the most important considerations is the inherent conductivity of the material.

Tellurium (Te), a sulfur element, has a higher conductivity compared with sulfur and selenium. It also has strong metallic characteristics, allowing telluride materials to admit more electrolyte ions and increase diffusion kinetics, enhancing energy storage reaction and offering

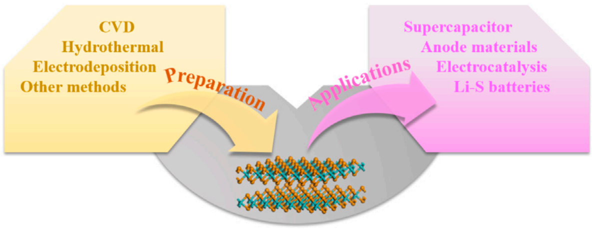

FIGURE 1
Overview framework of 2D metal telluride atomic crystals.

high rate capability of energy storage devices (Kshetri et al., 2021). Owing to the unusual electrical structures and various two-dimensional (2D) crystals of 2D metal tellurides, these materials have recently received widespread attention as an essential component of metal chalcogenides (Li et al., 2016; Apte et al., 2018; Kononov et al., 2020; Liu et al., 2020). For instance, VTe_2 has excellent electrocatalytic activity for hydrogen evolution reactions and is regarded as a high-performance electrode material (Shi et al., 2021). In addition, NiTe, which has better conductivity and faster electron transfer capability compared with semiconductors, can maintain a specific capacity of approximately 307 mAh g^{-1} at a high rate of 500 mA g^{-1} as the anode of rechargeable aluminum ion batteries (Yu et al., 2020). Thus, the study of cathode materials for aluminum ion batteries and their use as battery anode materials [e.g., $FeTe_2$ (Park and Kang, 2020) and $CoTe_2$ (Yang et al., 2020)], electrocatalytic materials [e.g., Ni_3Te_2 (De Silva et al., 2018) and $MoTe_2$ (Zhou et al., 2017a)], and SC materials [e.g., NiTe (Chen et al., 2019) and $CoTe_2$ (Manikandan et al., 2020)] is of great importance.

In recent years, tellurides have become widely used in electrochemistry owing to their 2D layered structure and unique properties (Wang et al., 2019; Li et al., 2020a; Myung et al., 2020; Zhang et al., 2021). On this basis, we provide a comprehensive overview of tellurides in this study, as shown in Figure 1. We first focus on the preparation methods of telluride electrode materials, including chemical vapor deposition (CVD) (Wood et al., 2014; Zhou et al., 2017b; Tang et al., 2019; Hao et al., 2021; Zhang et al., 2021; Zhou et al., 2021), hydrothermal method (Wang et al., 2012; Hou et al., 2013; Oh et al., 2020; Qi et al., 2021), and electrodeposition (Morris and Vanderveen, 1993; Yu et al., 2018), and their electrochemical properties and applications. Subsequently, conceivable perspectives on the challenges and opportunities of 2D telluride electrode materials are proposed to provide insights into future research.

2 Preparation

2D metal tellurides have recently become popular in energy devices such as SCs, photocatalysts, and electrode materials. Thus far, several preparation methods have been developed to synthesize 2D metal telluride nanomaterials, as summarized in Table 1.

2.1 Hydro/solvothermal methods

The most prevalent techniques for synthesizing nanomaterials are the hydrothermal and solvothermal procedures. In contrast to alternative procedures for synthesizing nanostructured materials, the hydrothermal approach offers the benefits of low synthesis temperature and small grain size. This approach may produce a wide range of morphologies, including nanorods (Yu et al., 2020; Jayababu et al., 2021), nanosheets (Lu et al., 2015; Li et al., 2020b), nanowires (Yang et al., 2009; Wan et al., 2011), and nanotubes (Wang et al., 2010). Moreover, in contrast to other synthesis methods, the hydrothermal approach has an excessively high oxygen affinity for positively charged metal and negatively charged Te ions, resulting in the formation of oxides. Reducing agents, such as hydrazine and sodium borohydride, are necessary to avoid oxide impurities in tellurides.

Wang et al. adopted the hydrothermal technique to synthesize Bi_2Te_3 nanotubes with diameters of 100 nm and lengths of 500–1,000 nm by using sodium borohydride as the reducing agent and EDTA as the surfactant (Figure 2A–D) (Wang et al., 2010). Zhang et al. created carbon-encapsulated porous Sb_2Te_3 nanoplates with porous architectures *via* the hydrothermal and carbonization processes, with carbon shell thicknesses ranging from 50 to 80 nm (Figures 2E–J) (Zhang et al., 2019b). Their approach can successfully produce nanomaterials, such as Ag_2Te (Zhang et al., 2006), Bi_2Te_3 (Wang et al., 2010), CdTe (Gong et al., 2011), Cu_2Te (Zhang et al., 2006), $Cu_{2\text{-}x}Te$ (Jamwal et al., 2016a), HgTe (Salavati-Niasari et al., 2010), NiTe (Zhang et al., 2002), and PbTe (Jamwal et al., 2016b).

Similar advantages can be attained in solvothermal reactions, such as when one or more precursors are dissolved in a non-aqueous solvent. The $BiSbTe_3$ nanosheets were prepared under solvent-heated conditions by using ethylene glycol as the solvent (Figures 2K–M) (Zhu et al., 2020). The unique nano-plate structure of $BiSbTe_3$ increases the exposure of the electrolyte, leading to high utilization of the composite electrode material during cycling. In addition, the solvothermal method is also commonly used to prepare other metal tellurides, such as Bi_2Te_3 (Liu et al., 2017a), Cu_xTe (Liu et al., 2017a), PbTe (Liu et al., 2017a), Ag_2Te (Liu et al., 2017a), and Sb_2Te_3 (Yan et al., 2016).

2.2 Chemical vapor deposition methods

CVD is generally used to create thin film materials. This approach is based on the principle of utilizing gaseous

TABLE 1 Synthesis methods and application of metal tellurides.

Tellurides	Applications	Preparation method	Morphology	Temp (°C)	Time (h)	Ref
Bi_2Te_3	-	Hydrothermal	Nanotubes	180	48	Wang et al. (2010)
	Thermoelectric application	Spark plasma sintering	Nanosheet	260	-	Kim et al. (2021)
$BiSbTe_3$	LIBs	Solvothermal	-	180	24	Zhu et al. (2020)
WTe_2	Superconductors	-	Film	350	-	Asaba et al. (2018)
$CoTe_2$	-	Solvothermal	Nanotubes	200	24	Li et al. (2009)
	Electrocatalyst	Hydrothermal	Nanoparticles	180	16	Lu et al. (2015)
	Li-S batteries	Hydrothermal	-	200	24	Song et al. (2021)
$MoTe_2$	Li-S batteries	Hydrothermal	-	200	36	Yu et al. (2021)
	Photocatalysts	Hydrothermal	-	200	48	Li et al. (2020b)
VTe_2	Li-S batteries	CVD	-	~650	-	Wang et al. (2019)
Sb_2Te_3	LIBs	Mixing	-	-	-	Grishanov et al. (2018a)
	-	Microwave-assisted Solvothermal	Various morphologies	-	-	Dong et al. (2011)
	LIBs	Ball milling	Micro-particles	-	12	Wei et al. (2020)
$Ge_2Sb_2T_5$	LIBs	Ball milling	-	-	40	Wei et al. (2019)
NiTe	Supercapacitor Electrode material	Solvothermal	Nanoplates	200	20	Chen et al. (2019)
		Hydrothermal	Network	180	18	Deshagani et al. (2020)
SnTe	LIBs	Hydrogen peroxide	-	-	-	Grishanov et al. (2018b)
Cu_2Te	-	Electrodeposition	-	-	-	Ishizaki et al. (2003)
$Cu_{(2-x)}Te$	Chemotherapy	Bio-synthesis	Nanocubes	160	0.75	Poulose et al. (2016)
ZnTe	Bio-imaging and bio-labeling	Bio-synthesis	Nanoparticles	-	-	Dunpall et al. (2014)
MnTe	Optoelectronic devices	CVD	Nanosheet	580	-	Li et al. (2020a)
In_2Te_3	Gas sensing and hydrogen storage	Solvothermal	Nanotubes	180	48	Zhou et al. (2014)

precursor reactants to produce thin films on a substrate by breaking down specific components of the gaseous precursor *via* atomic and intermolecular chemical interactions (Zhou et al., 2015; Naylor et al., 2016; Zhou et al., 2017b; Yoo et al., 2017). The form and properties of the 2D metal tellurides are influenced by the substrates, precursors, and temperature, among other factors (Zhou et al., 2016; Zhang et al., 2019c; Huang et al., 2019; Kim et al., 2020). CVD method is the most widely used method for the synthesis of tellurides, which has good scalability and can be controlled to prepare large-area films or two-dimensional crystals.

Recently, $MoTe_2$ has received widespread attention owing to its distinct semiconducting and semi-metallic characteristics. Kong et al. investigated a CVD technique for fabricating uniform high-crystalline 2H and 1T'-$MoTe_2$ films (Naylor et al., 2016). Various products were created by varying the precursor, carrier gas, and temperature. Under the same conditions, they observed that MoO_3 precursors converted more easily into 2H-$MoTe_2$, whereas MoO and MoO_x ($x < 3$) precursors converted more effectively into 1T'-$MoTe_2$. A year later, Kong et al. improved the preparation process and successfully synthesized large-size homogeneous 1T'-$MoTe_2$ (Zhou et al., 2016). They further determined the significant effect of the molybdenum precursor on the formation of 1T'-$MoTe_2$ (Figure 3A–E). 1T'-$MoTe_2$ was reliably created when MoO_3 was utilized as a precursor. Furthermore, the amount of Te used in the synthesis of 1T'-$MoTe_2$ had a substantial impact. If the Te supply is sufficient, then 2H-$MoTe_2$ would be produced; otherwise 1T'-$MoTe_2$ would be produced (Zhou et al., 2016). The established CVD technique also allowed for the large-scale direct synthesis of WTe_2 and $MoTe_2$ multilayers and monolayers (Zhou et al., 2017b). The thickness of the WTe_2 and $MoTe_2$ atomic layers was adjusted using growth time. (Figure 3F–M).

In addition to 2D WTe_2 and $MoTe_2$, many other 2D transition metal tellurides can be grown *via* CVD methods. Li et al. reported a method that can precisely control 2H-MoTe defects grown by a large-scale phase-change-assisted CVD process using selective etching of I_3^- solutions (Zhou et al., 2021). Liu et al. reported a facile CVD method to synthesize $Mo_xW_{1-x}Te_2$ with controlled thickness and chemical composition ratios to investigate its design of material devices from a topological quantum state perspective (Chubilleau et al., 2011). Li et al. reported a strategy using mixed molten salts for enhancing the CVD growth of 2D WTe_2 crystals with large grain size and yield, acting as a synergist (Jayababu et al., 2021).

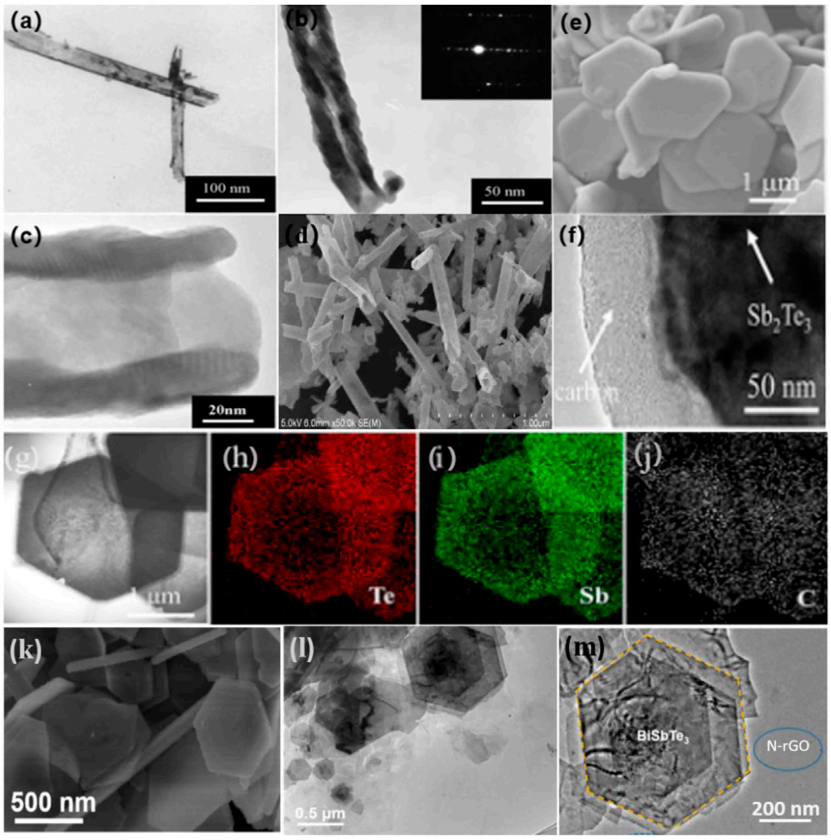

FIGURE 2
(A–D) TEM, SAED pattern, and SEM images of the Bi_2Te_3 (Wang et al., 2010). Copyright 2010, Elsevier. **(E–J)** morphologies and Te, Sb, C elemental mapping of the as-prepared Sb_2Te_3@C sample (Zhang et al., 2019b). Copyright 2019, American Chemical Society. **(K)** SEM of $BiSbTe_3$ nanosheets. **(L)** TEM and **(M)** HRTEM images of $BiSbTe_3$/N-rGO (Zhu et al., 2020). Copyright 2020, Elsevier.

2.3 Electrochemical deposition method

Electrochemical deposition (ECD) is another effective method for obtaining metal tellurides. ECD has the outstanding advantage of easily controlling the morphologies of metal tellurides by using removable templates. Compared with other methods, the ECD method is simple, not limited by grain size and shape, and the prepared crystalline materials have unique properties. Applied electrical potential and deposition rate are two critical parameters of smooth ECD.

Islam et al. suggested an ECD technique for handling bespoke Al_2O_3 (AAO) stencils that neither needed extensive hole branching nor would damage the aluminum substrate(Figure 4) (Wu et al., 2020). CdTe nanotubes have a high aspect ratio of one-dimensional nanostructures compared to other nanostructures and have amplified optical waveguide properties. Therefore, they are designed as visible light responsive photocatalysts. Figure 4A shows that CdTe was electrochemically deposited onto tailored AAO stencils, which has been sheared by utilizing the full AAO to allow for the acquisition of through-hole and self-supporting features on the Al substrate. The CdTe nanotubes developed in the sulfate bath after the barrier layer has been completely removed, as shown in Figure 4B. The image within the red border is a magnified view of the designated section in the red circle, revealing the hollow ends of the vertically aligned nanotubes. This feature implies the significant advantage of the material to provide electrical contact during cathodic deposition because the aluminum base remains intact even after the barrier layer is completely removed. Meanwhile, broaching barrier layer (BBL) was polarized in dilute H_2SO_4, compared to neutral KCl solution and immersion in H_3PO_4 solution, resulting in a totally etched barrier layer that was innocuous to the substrate aluminum.

Choa et al. converted Ag_2Te nanotubes to PbTe nanotubes by changing the silver-to-lead atomic ratio through the combined processes of electrostatic spinning, ECD, and cation exchange (Figures 5A–F) (Deshagani et al., 2020). Silver atoms were diffused into the Te layer and transformed into Ag_2Te nanofibers by ECD using silver nanofibers synthesized by

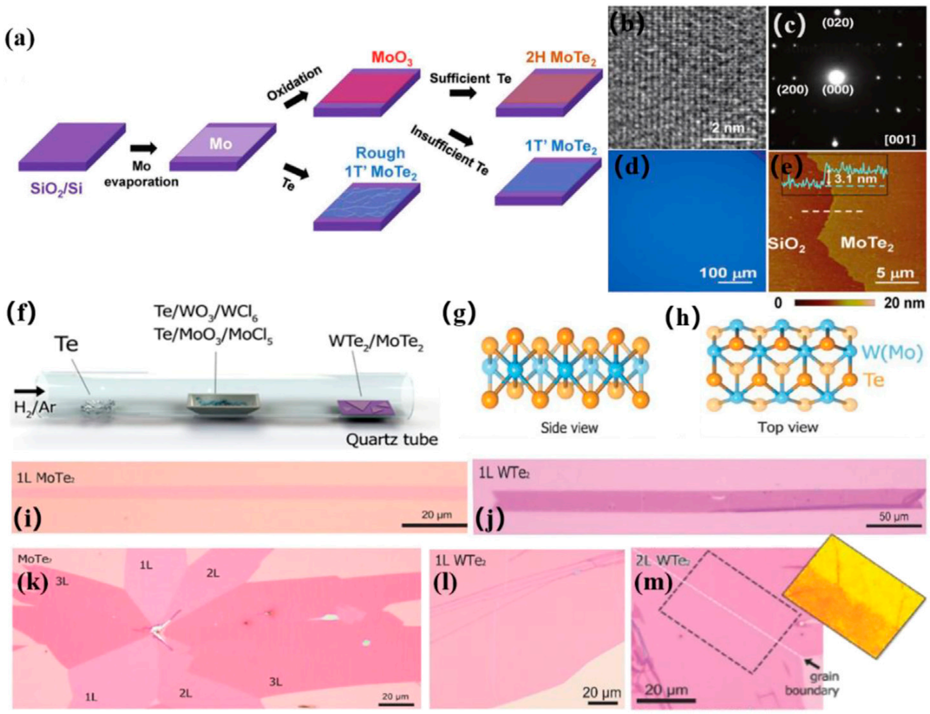

FIGURE 3
(A) Schematic illustration of CVD method to deposit 1T′ and 2H $MoTe_2$ films. **(B)** high-resolution TEM image, and **(C)** SAED pattern of 1T′- $MoTe_2$ film grown from MoO_3; **(D)** Typical optical and **(E)** AFM image of a 1T′- $MoTe_2$ film (Zhou et al., 2016). Copyright 2016, Wiley-VCH. **(F)** Schematic illustration of CVD method to grow WTe_2 and $MoTe_2$ atomic layers. **(G,H)** Crystalline structures of 1T′-W(Mo)Te_2. **(I,J)** Optical images of $MoTe_2$ and WTe_2 monolayer. **(K)** Optical image of a $MoTe_2$ flake containing 1, 2, and 3 L $MoTe_2$. **(L,M)** Optical images of a large scale monolayer and bilayer WTe_2 films (Zhou et al., 2017b). Copyright 2017, Wiley-VCH.

electrostatic spinning as the starting material. Then, the crystalline transition of Ag_xTe_y to PbTe nanocomposites was controlled by the cation exchange from Ag^+ cations to Pb^{2+} cations.

In addition to the abovementioned three methods, many other chemical routes can be used to extensively investigate the synthesis of metal telluride nanomaterials. Examples are microwave synthesis (Ye et al., 2019), spray pyrolysis (Chen et al., 2019), biosynthesis (Poulose et al., 2016), and laser ablation techniques (Jayababu and Kim, 2021). A good method allows for the accurate control of certain features, including spatial structure and distribution, which significantly impact the performance of electrode materials. Kang et al. investigated anode materials for potassium ion batteries using spray pyrolysis to make cobalt telluride-C ($CoTe_2$-C) composite microspheres, as shown in Figure 5G, (Yang et al., 2020). As Te needed to be directly embedded into the composite microspheres, a simple one-step post-treatment technique was used to prepare $CoTe_2$-C composite microspheres. Their approach could be explained by Ostwald maturation induced by the formation of the $CoTe_2$ crystals.

3 Applications as electrodes

3.1 Supercapacitor

Telluride has a substantially greater electrical conductivity and is projected to perform better electrochemically compared with other materials, leading to the widespread research and advancement of metal tellurides built into diverse nanostructures for supercapacitor (SC) applications (Liu et al., 2017b; Rathore et al., 2022). Kim et al. created silver-decorated NiFe alloy telluride nanorods (AMMT HNRs) on nickel foam (NF) (Figure 6A) (Jayababu et al., 2021). The robust electroactivity of the NiFe alloy, the high conductivity of Te and Ag, and the porous layered structure of the telluride all contributed to the AMMT HNRs/NF electrode's outstanding electrochemical performance. The electrode exhibited a stability of 80.4% over 3,000 cycles. After employing AMMT HNRs/NF and carbon-coated NF as positive and negative electrodes, respectively, and cellulose membranes as separators, high areal energy and power densities were reported in hybrid supercapacitors. (Figure 6B).

NiTe, as an SC electrode material, has also attracted the interest of scientists (Park et al., 2018; Song et al., 2021; Yu et al.,

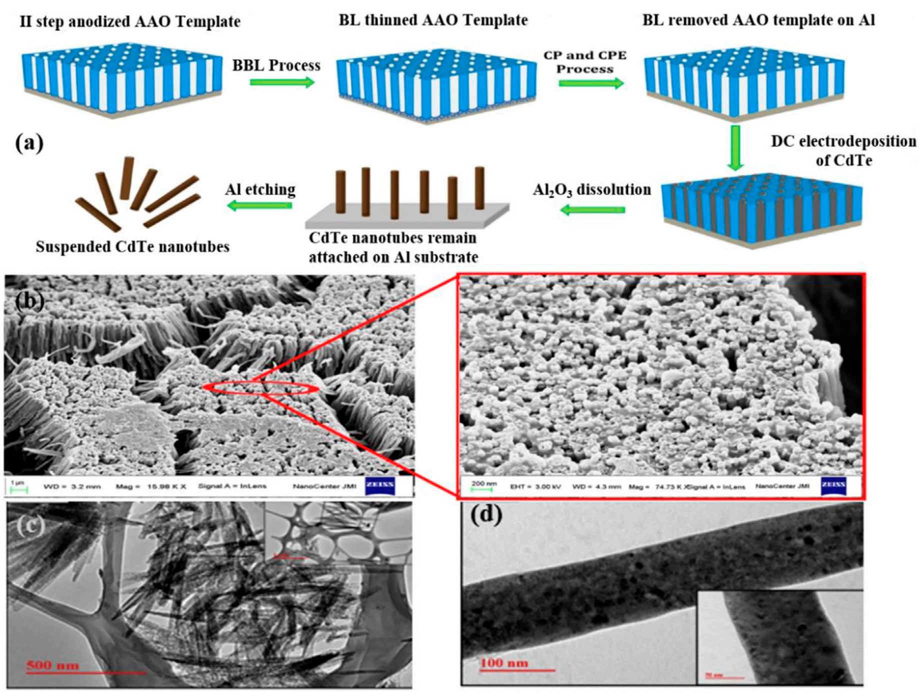

FIGURE 4
(A) Schematic illustration of the steps involved to remove barrier layer from AAO template keeping base Al intact for electrodeposition of CdTe nanotubes; and **(B)** FE-SEM micrograph of CdTe nanotubes deposited in BL removed AAO template. **(C)** TEM images illustrating CdTe hollow nanotubes; and **(D)** solid nanorod obtained using sulfate electrolyte bath (Wu et al., 2020). Copyright 2019, Elsevier.

2021). The NiTe achieved outstanding electrochemical performance as a coexisting pseudo capacitive material for NiS reported by Wu et al. (Chen et al., 2019). As shown in Figure 6D, four electrochemical reactions occurred on the NiS/NiTe/Ni (NST) electrode. During charging, the volume increased from the inner layer to the outer layer; during discharge, the volume was reduced from the outer layer to the inner layer. The NST was the positive electrode of the asymmetric SC, whereas the active carbon (AC) was the negative electrode. The high capacitance retention and ultra-long cycle life (200000 cycles, Figure 6E) demonstrated the important role of the synergistic structure to structural stability. Additionally, $CoTe_2$ (Manikandan et al., 2020), CuCoTe (Fu and Lee, 2019), VTe_2 (Ahmad et al., 2021), and $MoTe_2$ (Jin et al., 2018) have been widely used as electrode materials for high-performance capacitors.

3.2 Anode materials

Metal tellurides have emerged as the most feasible alternative for cutting-edge ion battery anode materials because to their layered crystal structure, high intrinsic conductivity, and high trap density (Zhu et al., 2020; Guo et al., 2021; Hassan et al., 2021). Kang et al. used a structurally distinct $FeTe_2$ and carbon nanocomposite as anode material for potassium ion batteries (Figure 7) (Park and Kang, 2020). The hollow carbon nanospheres that housed the iron telluride nanocrystals ($FeTe_2$-C) offered enough space to accommodate for the nanocrystals' enormous volume variations during charging and discharging. During cycling, nanocrystal extrusion within the solid hollow carbon nanospheres was controlled, and no $FeTe_2$ from the electrode were lost, showing strong structural integrity (Park and Kang, 2020). Kang et al. also investigated the reaction mechanism of the $CoTe_2$-C composite microsphere as an anode material for potassium ion batteries and the related potassium ion conversion. Where the mechanism of the $CoTe_2$ phase transition reaction can be expressed as:

$$2CoTe_2 + 7K^{+}7e^{-} \rightarrow 2Co + K_5Te_3 + K_2Te$$

$$2Co + K_5Te_3 + K_2Te \leftrightarrow 2CoTe + 2Te + 7K^{+}7e^{-}$$

The surface-driven reactions during rapid potassiumization/depotassiumization significantly promote the charge storage of $CoTe_2$-C in potassium ion cells, leading to excellent rate performance. And the high contribution of the capacitance-controlled behavior of $CoTe_2$-C indicates its good multiplicative performance. At

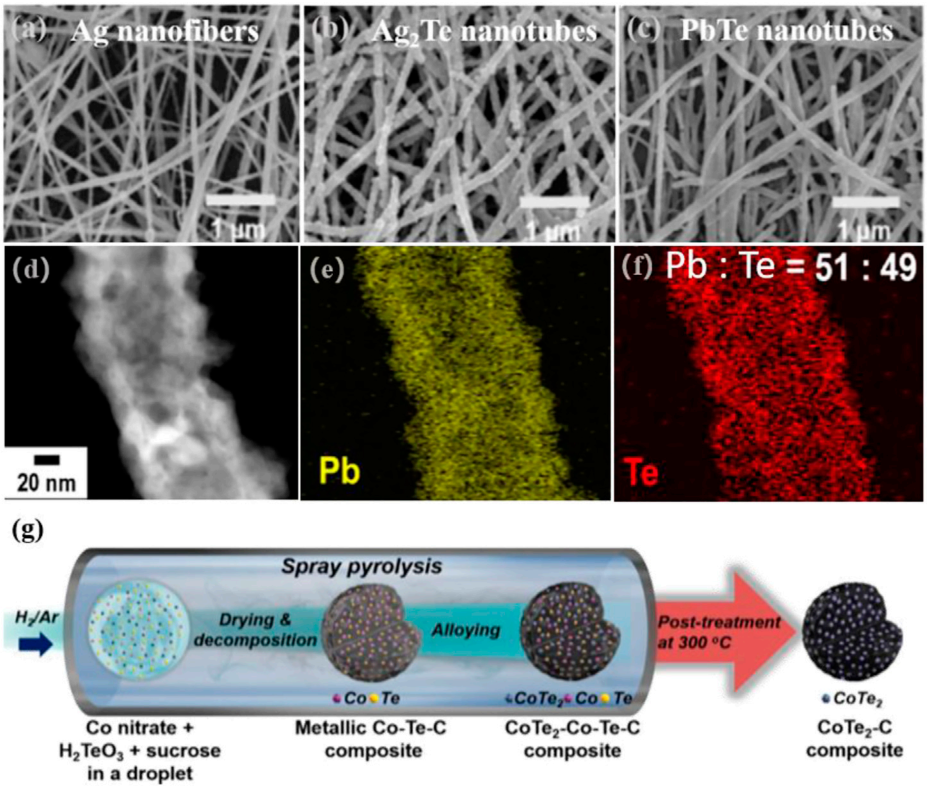

FIGURE 5
SEM images of **(A)** Ag nanofibers; **(B)** Ag_2Te nanotubes and **(C)** PbTe nanotubes; **(D–F)** EDS mapping (Deshagani et al., 2020). Copyright 2018, Elsevier. **(G)** Schematic illustration of the synthetic process of $CoTe_2$-C composite (Yang et al., 2020). Copyright 2020, Elsevier.

a current density of 0.5 A g^{-1}, the $CoTe_2$-C composite has a 100th cycle discharge capacity of 189.5 mAh g^{-1} (Chen et al., 2019). In addition, Kim et al. (Fu and Lee, 2019) investigated a CuCo LDHs-coated CuCoTe honeycomb nanosheet as anode for hybrid SCs. They demonstrated the material's excellent electrochemical performance and high stability (Chen et al., 2019).

3.3 Electrocatalysis

Depicted as 2D materials, tellurides have also been recently described as electrocatalytically active materials with low cost and strong catalytic activity (Luxa et al., 2017; Han et al., 2020). Nath et al. used hydrothermal and electrodeposition methods to create 5 and 8 nm-thick Ni_3Te_2 films (De Silva et al., 2018). Voltammetric cycling and linear sweep voltammetry were used to examine the OER catalytic activity of the as-synthesized materials in the alkaline electrolytes. Their results showed that Ni_3Te_2 films have a high catalytic efficiency of 10 mA cm^{-2} with a notably low overpotential of 180 mV. The overpotential value was much lower than that needed for nanostructured Ni_3Se_2 (190 mV) (Xu et al., 2019) and Ni_3S_2 (260 mV) (Li et al., 2022). Nanodendritic $MoTe_2$ was used as an electrocatalyst for hydrogen precipitation reaction (Zhou et al., 2017a). Nanodendrimers were created electrochemically on Mo-doped reduced polyimide/graphene oxide composite substrates. The deposition period increased the size of the nanodendrites. Their findings further showed that nanodendrimers have the potential to be good catalysts for hydrogen precipitation in neutral fluids. Ashiq et al. proposed a highly active Cu_7Te_4 nanowire synthesized through water oxidation as an electrocatalyst for water oxidation reaction (Zhang et al., 2022). Chu et al. demonstrated the ability of $FeTe_2$ to function as an efficient and durable nitrogen reduction electrocatalyst, with an excellent combination of NH_3 yield and Faraday efficiency (Yao et al., 2022). Metal telluride materials, such as Sb_2Te_3 (He et al., 2022), $MoTe_2$ [99], Ni_3Te_2-CoTe[100], and NiTe-$HfTe_2$[101], have received extensive attention for their potential application in electrocatalysis.

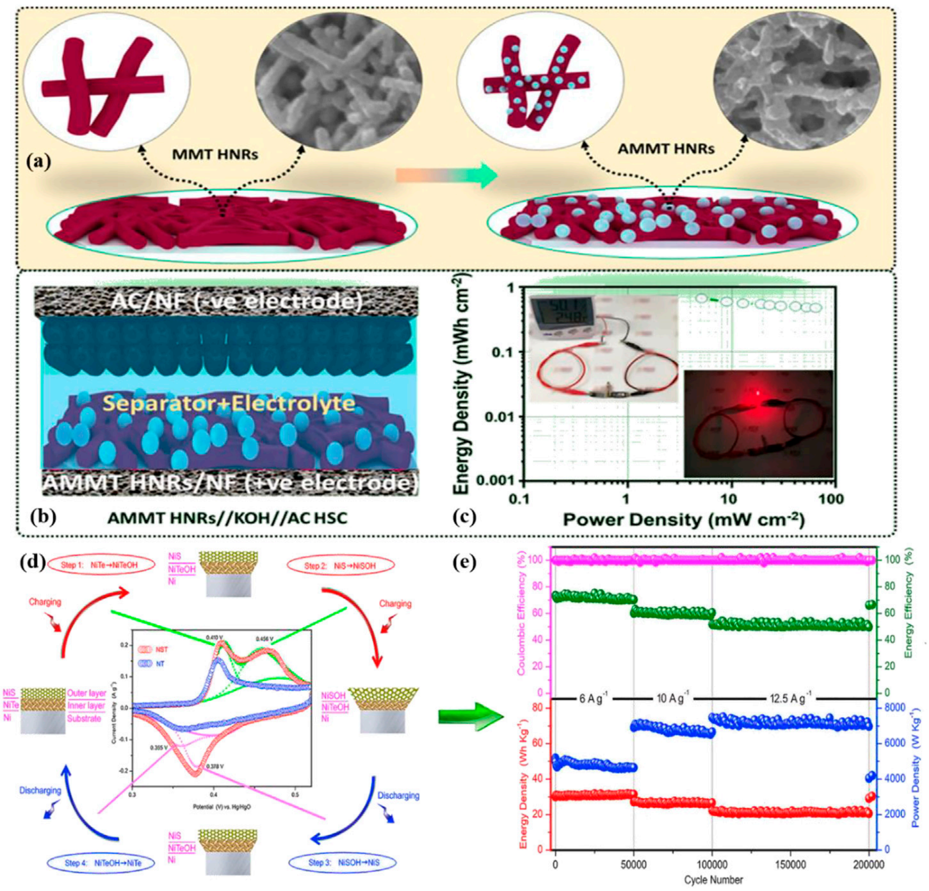

FIGURE 6
(A) Schematic of the MMT HNRs/NF and AMMT HNRs/NF electrodes; **(B)** Schematic of the hybrid supercapacitors; **(C)** Energy and power density of the hybrid supercapacitors and real-time suitability tests as a digital multi-sensor power supply (Jayababu et al., 2021). Copyright 2021, American Chemical Society. **(D)** Step by step illustration of NT and NST electrodes' electrochemical processes. **(E)** Electrochemical performance of NiS/NiTe/Ni//AC asymmetric supercapacitor electrodes up to over 200 000 cycles at different current densities (Chen et al., 2019). Copyright 2019, Elsevier.

3.4 Li-S batteries

Because of its low cost, environmental friendliness, and high energy density, Li-S batteries are appealing next-generation energy storage technologies. Meanwhile, owing to the intrinsic 2D structure of telluride, it offers an interesting function in Li-S batteries (Wang et al., 2019; Guo et al., 2021; Hassan et al., 2021).

Xie et al. examined diphenyl ditelluride (DPDTe) as bifunctional electrolyte additive for high-efficiency sulfur cathodes and dendrite-free lithium anodes[102]. As shown in Figures 8A–E, the presence of DPDTe enables catalytic mediation by Te radicals, which is accountable for substantially enhancing LIPS redox dynamics and regulating Li_2S accumulation. DPDTe can also combine with metallic lithium to generate a uniform, dense, and stable organic–inorganic hybrid SEI to minimize the nucleation overpotential of lithium and promote uniform lithium deposition, thereby successfully limiting the formation of lithium dendrites. The addition of DPDTe can improve sulfur usage and lead to highly reversible lithium stripping/plating, further resulting in good rate capability (611.4 mAh g^{-1} at 5C) of Li-S batteries.

Zhan et al. explored a phosphorus-doped nickel Te electrocatalyst ($P\subset NiTe_{2-x}$) grown on carbon-based (MSC) as a functional layer for high-performance Li-S battery separators ($MSC/P\subset NiTe_{2-x}$)[103]. The increased electrochemical performance implies that the P doping of Te vacancies can enhance Li-S battery conductivity, boost adsorption, and decrease the redox energy barrier of Li-S batteries. MSC nanosheets enable $NiTe_2$ nanoparticles to disperse and diffuse Li^+. *Ex-situ* X-ray absorption spectroscopy and *in-situ* Raman spectroscopy both demonstrated the ability of $MSC/P\subset NiTe_{2-x}$ to inhibit the shuttle effect and accelerate the redox conversion (Figures 8F–J). Compounding telluride materials in the electrode[91, 104], electrolyte, and diaphragm coatings has become one of the important strategies of breaking through the severe shuttle effect of Li-S batteries.

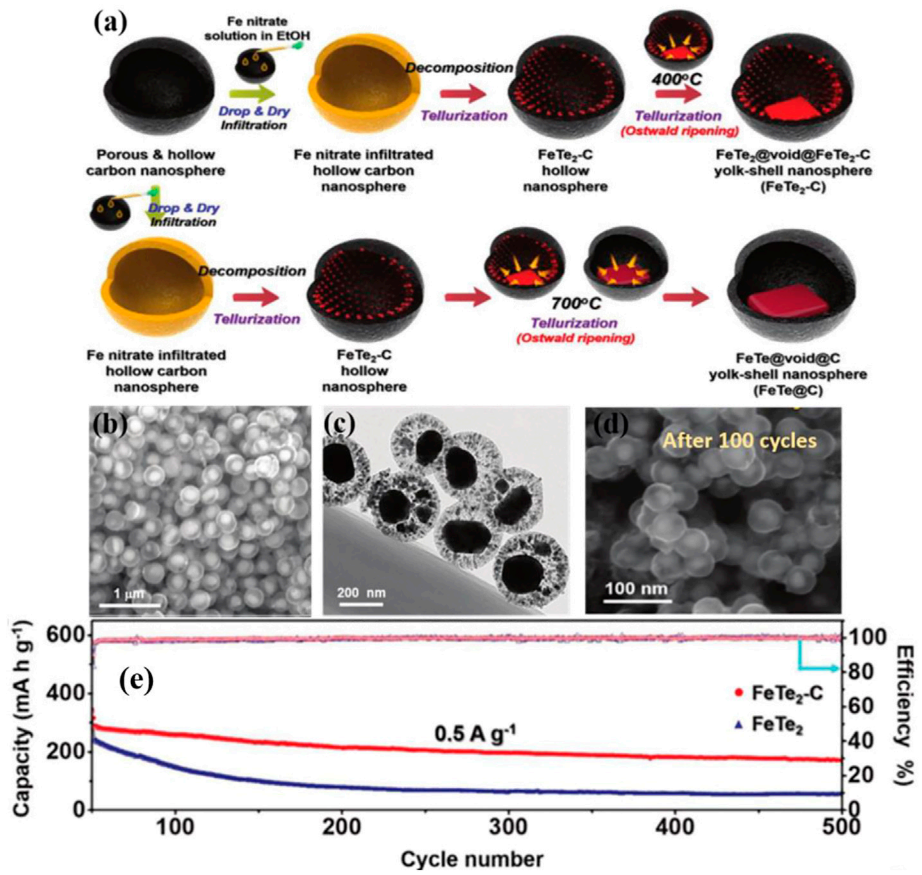

FIGURE 7
(A) Formation illustration of the hollow carbon nanosphere within $FeTe_2$-C nanospheres: **(B–D)** SEM and TEM images of initial $FeTe_2$-C and $FeTe_2$-C after cycled. **(E)** long-term cycling performances of $FeTe_2$ and $FeTe_2$-C (Park and Kang, 2020). Copyright 2020, Wiley-VCH.

4 Summary and prospective

Metal tellurides have received extensive attention owing to their great application potential for high-performance electrode materials. In this study, the synthesis methods of tellurides and the research progress of their properties and application in the field of electrodes were reviewed. Three methods for preparing metal tellurides were discussed. Then, the latest progress in terms of the role of telluride in capacitors, anode materials, electrocatalysis, and Li-S batteries was presented. Despite significant progress in the study of 2D tellurides, researchers still face considerable opportunities and challenges.

The CVD approach is now being widely utilized to controllably prepare tellurides. It is feasible to produce 2D tellurides with customizable shape and good crystallinity on a large scale. However, for powder electrochemical materials, the mild chemical interaction between the transition metal and Te under vapor conditions, on the other hand, is a disadvantage of CVD synthesis. Furthermore, while tellurides exhibit remarkable performance, they are difficult to precisely control properties such as pore structure and distribution in the preparation of electrode materials, which greatly affects the volume change of electrode materials during cycling, making it more difficult to improve the capacity, stability and extended cycle life of capacitors and batteries. Future studies should concentrate on: 1) investigating more approaches for the controlled synthesis of tellurides, not only for 2D single-crystal; and 2) designing more composites or building heterostructures to facilitate the electrochemical performances telluride-based electrodes, because like other sulfide generics, tellurides also suffer from extreme volume fluctuations, which result in poor cycling performance.

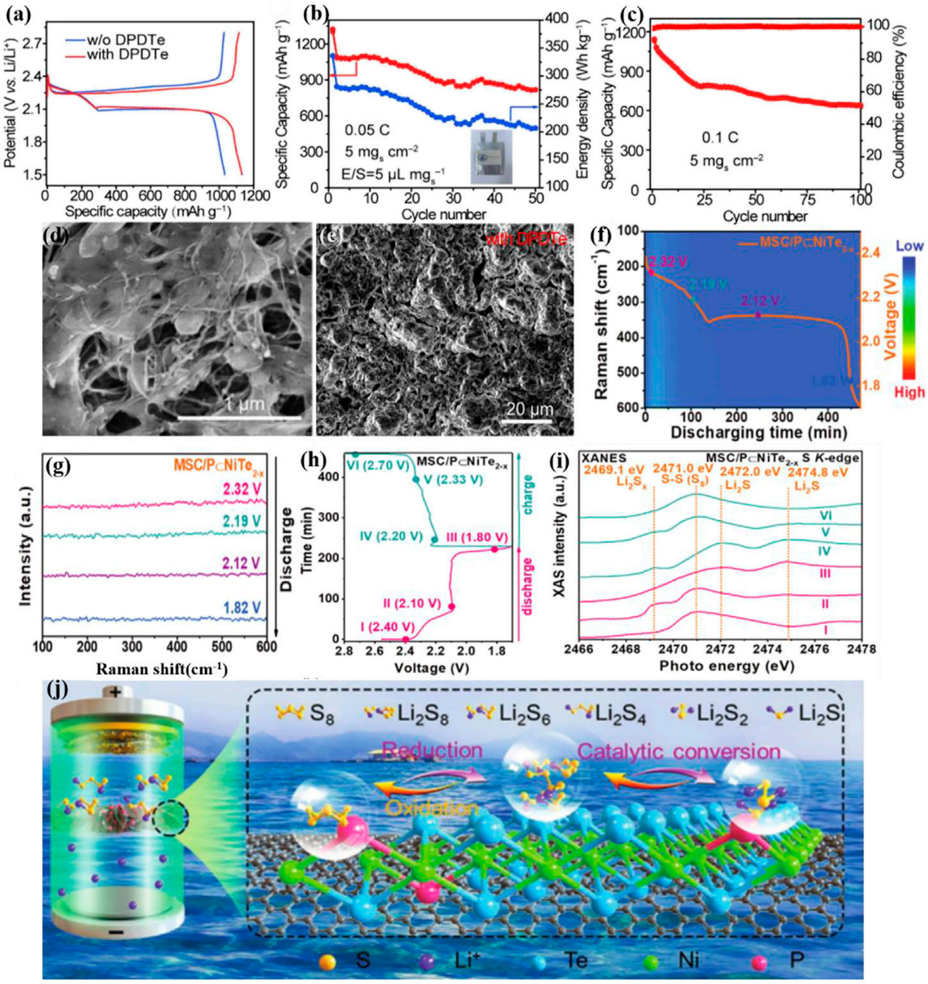

FIGURE 8
(A–C) Electrochemical performance of Li–S pouch cells with/without DPDTe additive, with high sulfur loading of 5 mg cm^{-2} and E/S ratio of 5.0 μL mg^{-1}. **(D)** SEM images of the Li_2S deposition with DPDTe and **(E)** the cycled Li anode with DPDTe additive at the 50th cycle[102]. Copyright 2022, Wiley-VCH. **(F,G)** *In situ* Raman contour plots and Raman spectra at 0.1 C with MSC/P⊂$NiTe_{2-x}$; **(H,I)** Galvanostatic discharge/charge profiles and corresponding *ex situ* XANES of the S K-edge cathode with MSC/P⊂$NiTe_{2-x}$ separator; **(J)** Adsorption-catalytic LiPS mechanism with MSC/P⊂$NiTe_{2-x}$ in a Li–S configuration[103]. Copyright 2022, Wiley-VCH.

Author contributions

MG: writing-original draft, investigation; SG: review and; editing, supervision, resources. SX: investigation, visualization, review and; editing; JL: visualization, review and; editing; YW: writing-review and; editing; GZ: resources, supervision.

Funding

This work was supported by the National Natural Science Foundation of China (Grant Nos. 22108133, 51972180, 51572134), the Program for Scientific Research Innovation Team in Colleges and Universities of Jinan (Grant No. 2018GXRC006), and Science, Education and Industry Integration of Basic Research Projects of Qilu University of Technology (Grant No. 2022PY062).

Conflict of interest

The authors declare that the research was conducted in the absence of any commercial or financial relationships that could be construed as a potential conflict of interest.

Publisher's note

All claims expressed in this article are solely those of the authors and do not necessarily represent those of their affiliated organizations, or those of the publisher, the editors and the reviewers. Any product that may be evaluated in this article, or claim that may be made by its manufacturer, is not guaranteed or endorsed by the publisher.

References

Ahmad, A., Khan, W. U., Shah, A. A., Yasin, N. A., Naz, S., Ali, A., et al. (2021). Synergistic effects of nitric oxide and silicon on promoting plant growth, oxidative stress tolerance and reduction of arsenic uptake in Brassica juncea. *Chemosphere* 262, 128384. doi:10.1016/j.chemosphere.2020.128384

Apte, A., Krishnamoorthy, A., Hachtel, J. A., Susarla, S., Idrobo, J. C., Nakano, A., et al. (2018). Telluride-based atomically thin layers of ternary two-dimensional transition metal dichalcogenide alloys. *Chem. Mat.* 30 (20), 7262–7268. doi:10.1021/acs.chemmater.8b03444

Asaba, T., Wang, Y., Li, G., Xiang, Z., Tinsman, C., Chen, L., et al. (2018). Magnetic field enhanced superconductivity in epitaxial thin film WTe_2. *Sci. Rep.* 8 (1), 6520–6527. doi:10.1038/s41598-018-24736-x

Chen, S., Wu, B., Qian, H., Wu, Z., Liu, P., Li, F., et al. (2019). An asymmetric supercapacitor using sandwich-like NiS/NiTe/Ni positive electrode exhibits a super-long cycle life exceeding 200 000 cycles. *J. Power Sources* 438, 227000. doi:10.1016/j.jpowsour.2019.227000

Chubilleau, C., Lenoir, B., Migot, S., and Dauscher, A. (2011). Laser fragmentation in liquid medium: A new way for the synthesis of PbTe nanoparticles. *J. colloid interface Sci.* 357 (1), 13–17. doi:10.1016/j.jcis.2011.01.057

De Silva, U., Masud, J., Zhang, N., Hong, Y., Liyanage, W. P. R., Asle Zaeem, M., et al. (2018). Nickel telluride as a bifunctional electrocatalyst for efficient water splitting in alkaline medium. *J. Mat. Chem. A Mat.* 6 (17), 7608–7622. doi:10.1039/c8ta01760c

Deshagani, S., Ghosal, P., and Deepa, M. (2020). Altered crystal structure of nickel telluride by selenide doping and a poly (N-methylpyrrole) coating amplify supercapacitor performance. *Electrochimica Acta* 345, 136200. doi:10.1016/j.electacta.2020.136200

Dong, G. H., Zhu, Y. J., and Chen, L. D. (2011). Sb_2Te_3 nanostructures with various morphologies: Rapid microwave solvothermal synthesis and seebeck coefficients. *CrystEngComm* 13 (22), 6811–6816. doi:10.1039/c1ce05591g

Dunpall, R., Mlowe, S., and Revaprasadu, N. (2014). Evidence of oriented attachment in the growth of functionalized ZnTe nanoparticles for potential applications in bio-imaging. *New J. Chem.* 38 (12), 6002–6007. doi:10.1039/c4nj01183j

Elmorshedy, M. F., Elkadeem, M. R., Kotb, K. M., Taha, I. B., and Mazzeo, D. (2021). Optimal design and energy management of an isolated fully renewable energy system integrating batteries and supercapacitors. *Energy Convers. Manag.* 245, 114584. doi:10.1016/j.enconman.2021.114584

Fu, G., and Lee, J. M. (2019). Ternary metal sulfides for electrocatalytic energy conversion. *J. Mat. Chem. A Mat.* 7 (16), 9386–9405. doi:10.1039/c9ta01438a

Gong, H., Hao, X., Wu, Y., Cao, B., Xu, H., and Xu, X. (2011). Influence of EDTA2− on the hydrothermal synthesis of CdTe nanocrystallites. *J. Solid State Chem.* 184 (12), 3269–3272. doi:10.1016/j.jssc.2011.10.018

Goodenough, J. B. (2014). Electrochemical energy storage in a sustainable modern society. *Energy Environ. Sci.* 7 (1), 14–18. doi:10.1039/c3ee42613k

Grishanov, D. A., Mikhaylov, A. A., Medvedev, A. G., Gun, J., Nagasubramanian, A., Madhavi, S., et al. (2018). Synthesis of high volumetric capacity graphene oxide-supported tellurantimony Na-and Li-ion battery anodes by hydrogen peroxide sol gel processing. *J. colloid interface Sci.* 512, 165–171. doi:10.1016/j.jcis.2017.10.040

Grishanov, D. A., Mikhaylov, A. A., Medvedev, A. G., Gun, J., Prikhodchenko, P. V., Xu, Z. J., et al. (2018). Graphene oxide-supported β-tin telluride composite for sodium-and lithium-ion battery anodes. *Energy Technol.* 6 (1), 127–133. doi:10.1002/ente.201700760

Guo, Y., Cheng, Y., Li, Q., and Chu, K. (2021). $FeTe_2$ as an earth-abundant metal telluride catalyst for electrocatalytic nitrogen fixation. *J. Energy Chem.* 56, 259–263. doi:10.1016/j.jechem.2020.07.055

Han, Y., Cai, W., Wu, X., Qi, W., Li, B., Li, H., et al. (2020). Electrocatalytic nitrogen fixation on metal tellurides boosted by multiple promoted-synergetic effects of telluride. *Cell Rep. Phys. Sci.* 1 (11), 100232. doi:10.1016/j.xcrp.2020.100232

Hao, Z., Xu, K., Kang, J., Chen, C., and Zhu, W. (2021). Atomically thin telluride multiheterostructures: Toward spatial modulation of bandgaps. *Nanoscale* 13 (46), 19587–19592. doi:10.1039/d1nr03746c

Hassan, A., Nisar, L., Iqbal, R., Sadaqat, M., Hussain, F., Ashiq, M. N., et al. (2021). Copper telluride nanowires for high performance electrocatalytic water oxidation in alkaline media. *J. Power Sources* 491, 229628. doi:10.1016/j.jpowsour.2021.229628

He, J., Bhargav, A., and Manthiram, A. (2022). *In situ* grown 1T′-$MoTe_2$ nanosheets on carbon nanotubes as an efficient electrocatalyst and lithium regulator for stable lithium–sulfur full cells. *Adv. Energy Mater.* 12 (1), 2103204. doi:10.1002/aenm.202103204

Hou, T. C., Yang, Y., Lin, Z. H., Ding, Y., Park, C., Pradel, K. C., et al. (2013). Nanogenerator based on zinc blende CdTe micro/nanowires. *Nano Energy* 2 (3), 387–393. doi:10.1016/j.nanoen.2012.11.004

Huang, W., Yin, L., Wang, F., Cheng, R., Wang, Z., Sendeku, M. G., et al. (2019). Multibit optoelectronic memory in top-floating-gated van der Waals heterostructures. *Adv. Funct. Mat.* 29 (36), 1902890. doi:10.1002/adfm.201902890

Ishizaki, T., Yata, D., and Fuwa, A. (2003). Electrodeposition of a copper-tellurium compound under diffusion-limiting control. *Mat. Trans.* 44 (8), 1583–1587. doi:10.2320/matertrans.44.1583

Jaiswal, A. (2017). Lithium-ion battery based renewable energy solution for off-grid electricity: A techno-economic analysis. *Renew. Sustain. Energy Rev.* 72, 922–934. doi:10.1016/j.rser.2017.01.049

Jamwal, D., Rana, D., Pathak, D., Raizada, P., and Thakur, P. (2016). Array of bis-quaternary ammonium surfactant tailored $Cu_{(2-x)}Te$ quantum dots with amended functional assets. *RSC Adv.* 6 (17), 13981–13990. doi:10.1039/c5ra24396c

Jamwal, D., Rana, D., Singh, P., Pathak, D., Kalia, S., Thakur, P., et al. (2016). Well-defined quantum dots and broadening of optical phonon line from hydrothermal method. *RSC Adv.* 6 (104), 102010–102014. doi:10.1039/c6ra19818j

Jayababu, N., Jo, S., Kim, Y., and Kim, D. (2021). Novel conductive Ag-decorated NiFe mixed metal telluride hierarchical nanorods for high-performance hybrid supercapacitors. *ACS Appl. Mat. Interfaces* 13 (17), 19938–19949. doi:10.1021/acsami.1c00506

Jayababu, N., and Kim, D. (2021). CuCo LDHs coated CuCoTe honeycomb-like nanosheets as a novel anode material for hybrid supercapacitors. *Small* 17 (36), 2102369. doi:10.1002/smll.202102369

Jin, T., Han, Q., Wang, Y., and Jiao, L. (2018). 1D nanomaterials: Design, synthesis, and applications in sodium–ion batteries. *Small* 14 (2), 1703086. doi:10.1002/smll.201703086

Kim, H., Johns, J. E., and Yoo, Y. (2020). Mixed-dimensional heterostructures: Mixed-dimensional in-plane heterostructures from 1D Mo_6Te_6 and 2D $MoTe_2$ synthesized by Te-flux-controlled chemical vapor deposition (Small 47/2020). *Small* 16 (47), 2070255. doi:10.1002/smll.202070255

Kim, J., Kang, H., Ahn, B., and Seo, H. (2021). Fluorine doping for improved thermoelectric properties of spark plasma sintered bismuth telluride. *J. Mater. Sci. Technol.* 90, 225–235. doi:10.1016/j.jmst.2021.02.035

Kononov, A., Abulizi, G., Qu, K., Yan, J., Mandrus, D., Watanabe, K., et al. (2020). One-dimensional edge transport in few-layer WTe2. *Nano Lett.* 20 (6), 4228–4233. doi:10.1021/acs.nanolett.0c00658

Kshetri, T., Singh, T. I., Lee, Y. S., Khumujam, D. D., Kim, N. H., and Lee, J. H. (2021). Metal organic framework-derived cobalt telluride-carbon porous structured composites for high-performance supercapacitor. *Compos. Part B Eng.* 211, 108624. doi:10.1016/j.compositesb.2021.108624

Li, H., Gu, S., Sun, Z., Guo, F., Xie, Y., Tao, B., et al. (2020). The in-built bionic "MoFe cofactor" in Fe-doped two-dimensional $MoTe_2$ nanosheets for boosting the photocatalytic nitrogen reduction performance. *J. Mat. Chem. A Mat.* 8 (26), 13038–13048. doi:10.1039/d0ta04251j

Li, J., Tang, X., Song, L., Zhu, Y., and Qian, Y. (2009). From Te nanotubes to $CoTe_2$ nanotubes: A general strategy for the formation of 1D metal telluride nanostructures. *J. Cryst. growth* 311 (20), 4467–4472. doi:10.1016/j.jcrysgro.2009.08.007

Li, L., Li, H., Li, J., Wu, H., Yang, L., Zhang, W., et al. (2020). Chemical vapor deposition-grown nonlayered α-MnTe nanosheet for photodetectors with ultrahigh responsivity and external quantum efficiency. *Chem. Mat.* 33 (1), 338–346. doi:10.1021/acs.chemmater.0c03898

Li, T., Wu, J., Qiao, L., Zhu, Q., Fu, Z., Lin, J., et al. (2022). Bimetallic Ni-Hf tellurides as an advanced electrocatalyst for overall water splitting with layered g-C_3N_4 modification. *Mater. Today Energy* 26, 101002. doi:10.1016/j.mtener.2022.101002

Li, Y., Duerloo, K. A. N., Wauson, K., and Reed, E. J. (2016). Structural semiconductor-to-semimetal phase transition in two-dimensional materials induced by electrostatic gating. *Nat. Commun.* 7 (1), 10671–10678. doi:10.1038/ncomms10671

Liu, C., Gao, H., Li, Y., Wang, K., Burton, L. A., and Ren, W. (2020). Manipulation of the Rashba effect in layered tellurides MTe (M= Ge, Sn, Pb). *J. Mat. Chem. C Mat.* 8 (15), 5143–5149. doi:10.1039/d0tc00003e

Liu, M., Wang, Z., Liu, J., Wei, G., Du, J., Li, Y., et al. (2017). Synthesis of few-layer 1T′-$MoTe_2$ ultrathin nanosheets for high-performance pseudocapacitors. *J. Mat. Chem. A Mat.* 5 (3), 1035–1042. doi:10.1039/c6ta08206h

Liu, S., Peng, N., Bai, Y., Xu, H., Ma, D. Y., Ma, F., et al. (2017). General solvothermal approach to synthesize telluride nanotubes for thermoelectric applications. *Dalton Trans.* 46 (13), 4174–4181. doi:10.1039/c7dt00085e

Lu, T. H., Chen, C. J., Basu, M., Ma, C. G., and Liu, R. S. (2015). The $CoTe_2$ nanostructure: An efficient and robust catalyst for hydrogen evolution. *Chem. Commun.* 51 (95), 17012–17015. doi:10.1039/c5cc06806a

Luxa, J., Vosecký, P., Mazánek, V., Sedmidubsky, D., Pumera, M., Lazar, P., et al. (2017). Layered transition-metal ditellurides in electrocatalytic applications contrasting properties. *ACS Catal.* 7 (9), 5706–5716. doi:10.1021/acscatal.7b02080

Manikandan, M., Subramani, K., Sathish, M., and Dhanuskodi, S. (2020). Hydrothermal synthesis of cobalt telluride nanorods for a high performance hybrid asymmetric supercapacitor. *RSC Adv.* 10 (23), 13632–13641. doi:10.1039/c9ra08692g

Morris, G. C., and Vanderveen, R. J. (1993). Cadmium telluride films prepared by pulsed electrodeposition. *Sol. energy Mater. Sol. cells* 30 (4), 339–351. doi:10.1016/0927-0248(93)90111-f

Myung, N., Park, H. Y., Jee, H. W., Sohn, E. B., Lee, S. J., Paeng, K. J., et al. (2020). Electrosynthesis of $MoTe_2$ thin films: A combined voltammetry-electrochemical quartz crystal microgravimetry study of mechanistic aspects. *J. Electrochem. Soc.* 167 (11), 116510. doi:10.1149/1945-7111/aba15e

Naylor, C. H., Parkin, W. M., Ping, J., Gao, Z., Zhou, Y. R., Kim, Y., et al. (2016). Monolayer single-crystal 1T′-$MoTe_2$ grown by chemical vapor deposition exhibits weak antilocalization effect. *Nano Lett.* 16 (7), 4297–4304. doi:10.1021/acs.nanolett.6b01342

Oh, J., Park, H. J., Bala, A., Kim, H. S., Liu, N., Choo, S., et al. (2020). Nickel telluride vertically aligned thin film by radio-frequency magnetron sputtering for hydrogen evolution reaction. *Apl. Mater.* 8 (12), 121104. doi:10.1063/5.0024588

Park, G. D., and Kang, Y. C. (2020). Conversion reaction mechanism for yolk-shell-structured iron telluride-C nanospheres and exploration of their electrochemical performance as an anode material for potassium-ion batteries. *Small Methods* 4 (10), 2000556. doi:10.1002/smtd.202000556

Park, J., Kwon, T., Kim, J., Jin, H., Kim, H. Y., Kim, B., et al. (2018). Hollow nanoparticles as emerging electrocatalysts for renewable energy conversion reactions. *Chem. Soc. Rev.* 47 (22), 8173–8202. doi:10.1039/c8cs00336j

Poulose, A. C., Veeranarayanan, S., Mohamed, M. S., Aburto, R. R., Mitcham, T., Bouchard, R. R., et al. (2016). Multifunctional $Cu_{2-x}Te$ nanocubes mediated combination therapy for multi-drug resistant MDA MB 453. *Sci. Rep.* 6 (1), 35961–36013. doi:10.1038/srep35961

Qi, Y., Yang, Z., Peng, S., Wang, M., Bai, J., Li, H., et al. (2021). Self-supported cobalt–nickel bimetallic telluride as an advanced catalyst for the oxygen evolution reaction. *Inorg. Chem. Front.* 8 (18), 4247–4256. doi:10.1039/d1qi00693b

Rathore, H. K., Hariram, M., Ganesha, M. K., Singh, A. K., Das, D., Kumar, M., et al. (2022). Charge storage mechanism in vanadium telluride/carbon nanobelts as electroactive material in an aqueous asymmetric supercapacitor. *J. Colloid Interface Sci.* 621, 110–118. doi:10.1016/j.jcis.2022.04.062

Salavati-Niasari, M., Bazarganipour, M., and Davar, F. (2010). Solution-chemical syntheses of nanostructure HgTe via a simple hydrothermal process. *J. Alloys Compd.* 499 (1), 121–125. doi:10.1016/j.jallcom.2010.03.135

Shi, J., Huan, Y., Zhao, X., Yang, P., Hong, M., Xie, C., et al. (2021). Two-dimensional metallic vanadium ditelluride as a high-performance electrode material. *ACS Nano* 15 (1), 1858–1868. doi:10.1021/acsnano.0c10250

Song, X., Tian, D., Qiu, Y., Sun, X., Jiang, B., Zhao, C., et al. (2021). Efficient polysulfide trapping and conversion on N-doped $CoTe_2$ via enhanced dual-anchoring effect. *Small* 17 (42), 2102962. doi:10.1002/smll.202102962

Tang, B., Zhou, J., Sun, P., Wang, X., Bai, L., Dan, J., et al. (2019). Phase-controlled synthesis of monolayer ternary telluride with a random local displacement of tellurium atoms. *Adv. Mat.* 31 (23), 1900862. doi:10.1002/adma.201900862

Wan, B., Hu, C., Zhou, W., Liu, H., and Zhang, Y. (2011). Construction of strong alkaline hydrothermal environment for synthesis of copper telluride nanowires. *Solid state Sci.* 13 (10), 1858–1864. doi:10.1016/j.solidstatesciences.2011.07.018

Wang, B. B., Zhu, M. K., Wang, H., Dong, G., and Xie, H. (2012). Study on effects of sodium hydroxide on synthesis of zinc telluride nanocrystals by hydrothermal method. *Mater. Sci. Semicond. Process.* 15 (2), 131–135. doi:10.1016/j.mssp.2011.09.003

Wang, M., Song, Y., Sun, Z., Shao, Y., Wei, C., Xia, Z., et al. (2019). Conductive and catalytic VTe_2@ MgO heterostructure as effective polysulfide promotor for lithium–sulfur batteries. *ACS Nano* 13 (11), 13235–13243. doi:10.1021/acsnano.9b06267

Wang, Z., Wang, F., Chen, H., Zhu, L., Yu, H. j., and Jian, X. y. (2010). Synthesis and characterization of Bi_2Te_3 nanotubes by a hydrothermal method. *J. alloys Compd.* 492 (1-2), L50–L53. doi:10.1016/j.jallcom.2009.11.155

Wei, Y., Chen, J., Wang, S., Zhong, X., Xiong, R., Gan, L., et al. (2020). Wrapping Sb_2Te_3 with a graphite layer toward high volumetric energy and long cycle Li-ion batteries. *ACS Appl. Mat. Interfaces* 12 (14), 16264–16275. doi:10.1021/acsami.9b22346

Wei, Y., Huang, L., Chen, J., Guo, Y., Wang, S., Li, H., et al. (2019). Level the conversion/alloying voltage gap by grafting the endogenetic Sb_2Te_3 building block into layered GeTe to build $Ge_2Sb_2Te_5$ for Li-ion batteries. *ACS Appl. Mat. Interfaces* 11 (44), 41374–41382. doi:10.1021/acsami.9b14293

Wood, S. M., Klavetter, K. C., Heller, A., and Mullins, C. B. (2014). Fast lithium transport in PbTe for lithium-ion battery anodes. *J. Mat. Chem. A Mat.* 2 (20), 7238–7243. doi:10.1039/c4ta01167h

Wu, B., Qian, H., Nie, Z., Luo, Z., Wu, Z., Liu, P., et al. (2020). Ni_3S_2 nanorods growing directly on Ni foam for all-solid-state asymmetric supercapacitor and efficient overall water splitting. *J. Energy Chem.* 46, 178–186. doi:10.1016/j.jechem.2019.11.011

Xu, J., Yin, Y., Xiong, H., Du, X., Jiang, Y., Guo, W., et al. (2019). Improving catalytic activity of metal telluride by hybridization: An efficient Ni3Te2-CoTe composite electrocatalyst for oxygen evolution reaction. *Appl. Surf. Sci.* 490, 516–521. doi:10.1016/j.apsusc.2019.06.080

Yan, X., Zheng, W., Liu, F., Yang, S., and Wang, Z. (2016). Thickness effects for thermoelectric property of antimony telluride nanoplatelets via solvothermal method. *Sci. Rep.* 6 (1), 37722–37728. doi:10.1038/srep37722

Yang, S., Park, G. D., and Kang, Y. C. (2020). Conversion reaction mechanism of cobalt telluride-carbon composite microspheres synthesized by spray pyrolysis process for K-ion storage. *Appl. Surf. Sci.* 529, 147140. doi:10.1016/j.apsusc.2020.147140

Yang, Y., Taggart, D. K., Brown, M. A., Xiang, C., Kung, S. C., Yang, F., et al. (2009). Wafer-scale patterning of lead telluride nanowires: Structure, characterization, and electrical properties. *ACS Nano* 3 (12), 4144–4154. doi:10.1021/nn901173p

Yao, W., Tian, C., Yang, C., Xu, J., Meng, Y., Manke, I., et al. (2022). P-doped $NiTe_2$ with Te-vacancies in lithium–sulfur batteries prevents shuttling and promotes polysulfide conversion. *Adv. Mater.* 34 (11), 2106370. doi:10.1002/adma.202106370

Ye, B., Gong, C., Huang, M., Ge, J., Fan, L., Lin, J., et al. (2019). A high-performance asymmetric supercapacitor based on Ni_3S_2-coated NiSe arrays as positive electrode. *New J. Chem.* 43 (5), 2389–2399. doi:10.1039/c8nj05399e

Yoo, Y., DeGregorio, Z. P., Su, Y., Koester, S. J., and Johns, J. E. (2017). In-plane 2H-1T′ $MoTe_2$ homojunctions synthesized by flux-controlled phase engineering. *Adv. Mat.* 29 (16), 1605461. doi:10.1002/adma.201605461

Yu, B., Huang, A., Srinivas, K., Zhang, X., Ma, F., Wang, X., et al. (2021). Outstanding catalytic effects of 1T′-$MoTe_2$ quantum dots@ 3D graphene in shuttle-free Li–S batteries. *ACS Nano* 15 (8), 13279–13288. doi:10.1021/acsnano.1c03011

Yu, Z., Ferrer-Argemi, L., Kim, J., Lim, J. H., Myung, N. V., and Lee, J. (2018). Phase-dependent thermal conductivity of electrodeposited antimony telluride films. *J. Mat. Chem. C Mat.* 6 (13), 3410–3416. doi:10.1039/c8tc00140e

Yu, Z., Jiao, S., Tu, J., Luo, Y., Song, W. L., Jiao, H., et al. (2020). Rechargeable nickel telluride/aluminum batteries with high capacity and enhanced cycling performance. *ACS Nano* 14 (3), 3469–3476. doi:10.1021/acsnano.9b09550

Zeng, Y., Wang, M., He, W., Fang, P., Wu, M., Tong, Y., et al. (2019). Engineering high reversibility and fast kinetics of Bi nanoflakes by surface modulation for ultrastable nickel–bismuth batteries. *Chem. Sci.* 10 (12), 3602–3607. doi:10.1039/c8sc04967j

Zhang, H. T., Xiong, Y. M., Luo, X. G., Wang, C., Li, S., and Chen, X. (2002). Hydrothermal synthesis and characterization of NiTe alloy nanocrystallites. *J. Cryst. growth* 242 (3-4), 259–262. doi:10.1016/s0022-0248(02)01456-2

Zhang, L., Ai, Z., Jia, F., Liu, L., Hu, X., and Yu, J. C. (2006). Controlled hydrothermal synthesis and growth mechanism of various nanostructured films of copper and silver tellurides. *Chem. Eur. J.* 12 (15), 4185–4190. doi:10.1002/chem.200501404

Zhang, Q., and Guo, S. (2020). Emerging materials methods for renewable energy. *Small Methods* 4 (6), 2000087. doi:10.1002/smtd.202000087

Zhang, S., Qiu, L., Zheng, Y., Shi, Q., Zhou, T., Sencadas, V., et al. (2021). Rational design of core-shell ZnTe@ N-doped carbon nanowires for high gravimetric and volumetric alkali metal ion storage. *Adv. Funct. Mat.* 31 (3), 2006425. doi:10.1002/adfm.202006425

Zhang, W., Ma, F., Wu, Q., Zeng, Z., Zhong, W., Cheng, S., et al. (2022). A dual–functional organotelluride additive for highly efficient sulfur redox kinetics and lithium regulation in lithium–sulfur batteries. *Energy & Environ. Mater*. doi:10.1002/eem2.12369

Zhang, W., Zhang, Q., Shi, Q., Xin, S., Wu, J., Zhang, C. L., et al. (2019). Facile synthesis of carbon-coated porous Sb_2Te_3 nanoplates with high alkali metal ion storage. *ACS Appl. Mat. Interfaces* 11 (33), 29934–29940. doi:10.1021/acsami.9b09056

Zhang, X., Jin, Z., Wang, L., Hachtel, J. A., Villarreal, E., Wang, Z., et al. (2019). Low contact barrier in 2H/1T′ $MoTe_2$ in-plane heterostructure synthesized by chemical vapor deposition. *ACS Appl. Mat. Interfaces* 11 (13), 12777–12785. doi:10.1021/acsami.9b00306

Zhang, Y., Tang, Y., Deng, J., Leow, W. R., Xia, H., Zhu, Z., et al. (2019). Correlating the Peukert's constant with phase composition of electrode materials in fast lithiation processes. *ACS Mat. Lett.* 1 (5), 519–525. doi:10.1021/acsmaterialslett.9b00320

Zheng, G., Wang, D., Tian, S., Ren, M., and Song, M. (2021). Effect of microstructure and contact interfaces of cobalt MOFs-derived carbon matrix composite electrode materials on lithium storage performance. *Energy* 222, 119914. doi:10.1016/j.energy.2021.119914

Zhou, J., Liu, F., Lin, J., Huang, X., Xia, J., Zhang, B., et al. (2017). Large-area and high-quality 2D transition metal telluride. *Adv. Mat.* 29 (3), 1603471. doi:10.1002/adma.201603471

Zhou, L., Xu, K., Zubair, A., Liao, A. D., Fang, W., Ouyang, F., et al. (2015). Large-area synthesis of high-quality uniform few-layer $MoTe_2$. *J. Am. Chem. Soc.* 137 (37), 11892–11895. doi:10.1021/jacs.5b07452

Zhou, L., Yan, S., Lu, T., Shi, Y., Wang, J., and Yang, F. (2014). Indium telluride nanotubes: Solvothermal synthesis, growth mechanism, and properties. *J. Solid State Chem.* 211, 75–80. doi:10.1016/j.jssc.2013.11.033

Zhou, L., Zubair, A., Wang, Z., Zhang, X., Ouyang, F., Xu, K., et al. (2016). Synthesis of high-quality large-area homogenous 1T′ $MoTe_2$ from chemical vapor deposition. *Adv. Mat.* 28 (43), 9526–9531. doi:10.1002/adma.201602687

Zhou, Y., Jia, L., Feng, Q., Wang, T., Li, X., and Wang, C. (2017). $MoTe_2$ nanodendrites based on Mo doped reduced graphene oxide/polyimide composite film for electrocatalytic hydrogen evolution in neutral solution. *Electrochimica Acta* 229, 121–128. doi:10.1016/j.electacta.2017.01.147

Zhou, Y., Tao, L., Chen, Z., Lai, H., Xie, W., and Xu, J. (2021). Defect etching of phase-transition-assisted CVD-grown 2H-$MoTe_2$. *Small* 17 (32), 2102146. doi:10.1002/smll.202102146

Zhu, Y., Zhao, J., Li, L., Mao, J., Xu, J., and Jin, J. (2020). One-step solvothermal synthesis of $BiSbTe_3$/N-doped reduced graphene oxide composite as lithium-ion batteries anode materials. *Chem. Eng. Sci.* 225, 115829. doi:10.1016/j.ces.2020.115829